

**Supporting information for: Polarization domain dynamics of barium titanate ultrathin films using piezoresponse force microscopy**

M. Zamani-Alavijeh,<sup>1,2</sup> T. Al. Morgan,<sup>2</sup> A. Kuchuk,<sup>2</sup> and G.J. Salamo<sup>1,2</sup>

<sup>1)</sup> *University of Arkansas, Physics Department, Fayetteville, AR, United States*

<sup>2)</sup> *University of Arkansas, Institute for Nanoscience and Engineering, Fayetteville, AR, United States*

(Dated: 9 March 2021)

There are 4 sections in the supporting information: A. Development of equation 5, B. Specification of the AFM tips, given by the manufacturer and confirmed using AFM measurement on a reference sample (TGT1), C. Development of equation 6, and D. The electric field in the film from COMSOL simulations.

## A. DEVELOPMENT OF EQUATION 5 FOR THE ELECTRIC FIELD IN THE FERROELECTRIC FILM.

Spherical coordinate system was used to approximate the electric field in the ferroelectric thin film between a conductive tip and a conductive substrate at lateral distances greater than about one tip diameter from the tip-surface contact (origin). The geometry and the parameters of the structure were described in Fig. 1. In the approximation for the electric field in the film, the lateral size of the film and the cone is assumed to be infinite. The spherical part of the tip is neglected when we are considering lateral distances,  $r$ , greater than about one tip diameter from the origin. The film is assumed to be thin compared to the lateral distance, and the electric field in the film is also assumed to be uniform in the film. Due to the symmetry in Fig. 1, the three-dimensional Laplace equation in spherical coordinate can be reduced to:

$$\nabla^2\phi = \frac{1}{r^2 \sin\theta} \frac{\partial}{\partial\theta} (\sin\theta \frac{\partial\phi}{\partial\theta}) = 0 \quad (\text{S1})$$

The solution for the differential equation is:

$$\frac{\partial\phi}{\partial\theta} = \frac{A}{\sin\theta} \quad \phi = A \ln \left| \tan \frac{\theta}{2} \right| + B \quad (\text{S2})$$

Where A and B are integration constants. The electric field is in the  $\theta$ -direction and given by:

$$E_\theta = \frac{-1}{r} \frac{\partial\phi}{\partial\theta} = \frac{-1}{r} \frac{A}{\sin\theta} \quad (\text{S3})$$

The electric field in the air and the film are therefore given by:

$$E_\theta^{air} = \frac{-1}{r} \frac{A_1}{\sin\theta} \quad (\text{S4})$$

$$E_\theta^{film} = \frac{-1}{r} \frac{A_2}{\sin\theta} \quad (\text{S5})$$

To find  $A_2$  in Eq. S5, the electric field in the film, we make use of two boundary conditions<sup>1</sup>:

$$\epsilon^{air} E_\theta^{air}(\pi/2) = \epsilon^{film} E_\theta^{film}(\pi/2) \quad (\text{S6})$$

$$- \int_{\theta_0}^{\pi/2} E_\theta^{air} r d\theta - \int_0^{-d} E_z^{film} dz = V \quad (\text{S7})$$

Here,  $d$  is thickness of the film,  $\theta_0$  is the cone half angle as shown in the Fig. 1 and  $E_\theta^{film}$  is approximately in the z-direction and equivalent to  $E_z^{film}$  for thin films. In the case where a

thin dielectric layer forms on the surface<sup>2-4</sup>, the change in the electric field due to the cone is negligible. Since  $\epsilon_{film}$  for BTO is much greater than  $\epsilon_{air}$ , we can neglect  $E_{film}^z$  in Eq. S7 and find  $A_2$  as

$$A_2 = \frac{-V\epsilon^{air}}{\epsilon^{film} \ln \left| \tan \frac{\theta_0}{2} \right|} \quad (S8)$$

Therefore, the magnitude of the electric field due to the cone in the film is approximated as:

$$E_z^{film} = \frac{1}{r \sin \theta} \frac{V\epsilon^{air}}{\left| \ln \left| \tan \frac{\theta_0}{2} \right| \right| \epsilon^{film}} \quad (S9)$$

By putting  $\epsilon^{air} = 1$  and  $\theta = \pi/2$ , the equation for the electric field perpendicular to the film at distances greater than about one tip diameter and larger than thickness of the film is given by:

$$E_z^{film} = \frac{1}{r} \frac{V}{\left| \ln \left| \tan \frac{\theta_0}{2} \right| \right| \epsilon^{film}} \quad (S10)$$

BTO is an anisotropic dielectric<sup>5</sup> with  $\epsilon_c \approx 200$  and  $\epsilon_a \approx 4000$ . Since the electric field in the film away from the tip is mostly in z-direction, the c-dielectric constant,  $\epsilon_c$ , is taken for  $\epsilon_{film}$ . The cone of the tip is a truncated cone so we need to transform  $r$  to  $r - r_0$  that  $r_0$  is the distance of the intercept of the cone with the surface from the origin. By considering these substitutions Eq. S10 results in the Eq. 5 in the paper.

## B. SPECIFICATION OF THE AFM TIPS, GIVEN BY THE MANUFACTURER AND CONFIRMED USING AFM MEASUREMENT ON A REFERENCE SAMPLE (TGT1).

The geometry of the tip, including the angle of the cone,  $\theta_0$ , the radius of tip apex,  $a$ , as well as the intercept of the cone of the tip with the surface,  $r_0$ , are needed to find the applied electric field from the AFM tip.

To find these parameters we used a reference sample patterned with pointed structures having a 10 nm apex radius and 500 nm height which was used to form an AFM image using our AFM tip as shown in Fig. S1. This was then used to deconvolve out the tip parameters shown in Fig. S2. The results for “tip #1 measured” and “tip #2 measured” are compared with the “tip specifications” given by the company in Table S1.

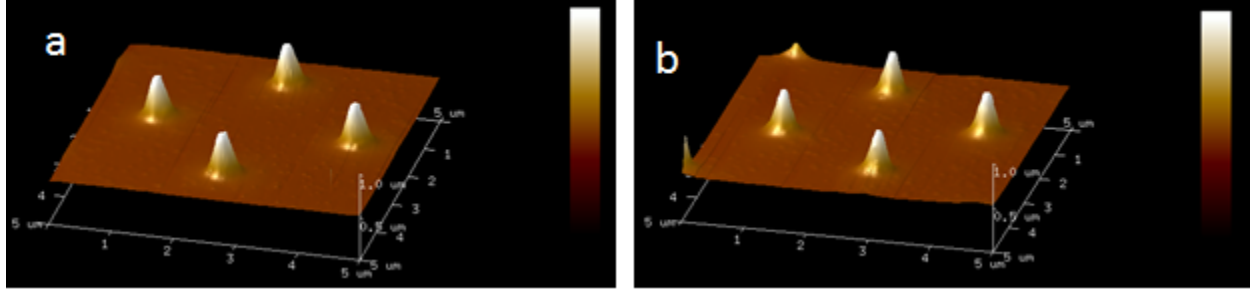


FIG. S1. 3-D AFM image of TGT1 sample with (a) tip#1, (b) tip#2. The image is  $5 \times 5 \mu\text{m}$ , the height scale is  $1 \mu\text{m}$ .

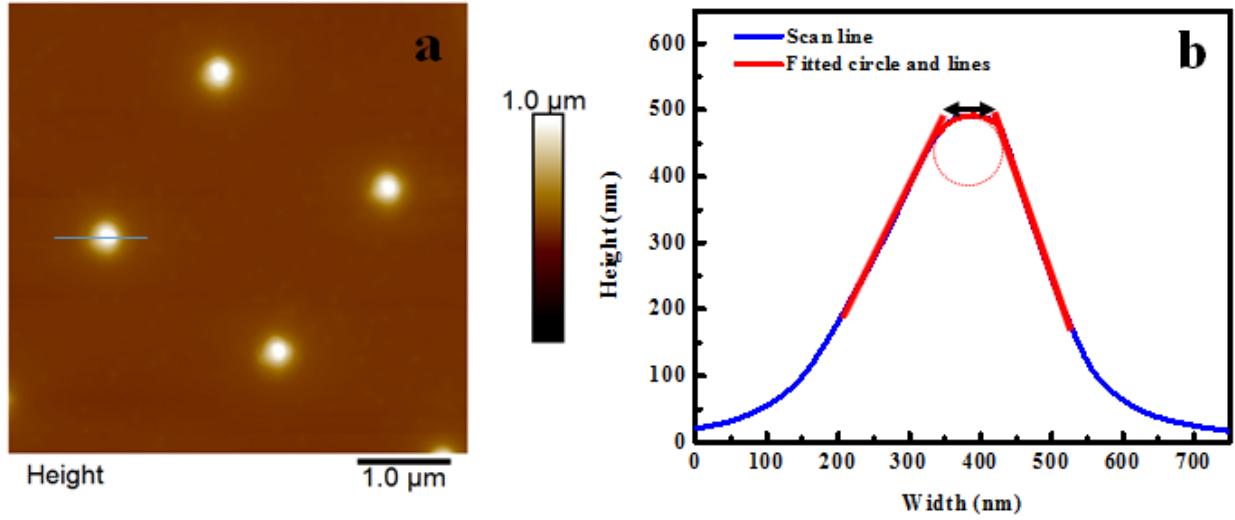


FIG. S2. (a) 2-D AFM image of TGT1 sample using tip#1, blue lines is a scan line. (b) Profile of the scan line of the AFM image, the radius of the fitted circle minus the radius of TGT1 is taken as radius of the AFM tip. Half of the double arrow length minus the radius of TGT1 is taken as  $r_0$ .

TABLE S1. Tip geometry specification and measured values by TGT1 sample.

-	$a(\text{nm})$	$\theta_0$	$r_0(\text{nm})$
Tip specification	20-50	$20^\circ$	-
Tip#1 measured	60	$20^\circ$	45
Tip#2 measured	30	$20^\circ$	20

### C. DEVELOPMENT OF EQUATION 6

To find the equation that describes the domain radius as a function of the poling time, the electric field (Eq. 5) is substituted into Merz's law (Eq. 2), and the velocity of domain wall is written as  $dr/dt$  in which  $r$  is the domain radius and  $t$  the poling time. Therefore, we have:

$$\frac{dr}{dt} = v_{\infty} \exp\left(-\frac{|\ln|\tan\frac{\theta_0}{2}||\epsilon_c E_a}{V}(r - r_0)\right) \quad (\text{S11})$$

To simplify the calculation we define  $\gamma$  as:

$$\gamma = \frac{V}{|\ln|\tan\frac{\theta_0}{2}||\epsilon_c} \quad (\text{S12})$$

Separating  $r$  and  $t$  terms on the two sides of equation (S11) gives:

$$\exp\left(-\frac{E_a}{\gamma}r_0\right)\exp\left(\frac{E_a}{\gamma}r\right)dr = v_{\infty}dt \quad (\text{S13})$$

Now we can integrate both sides with the initial values of  $(t_i, r_i)$  and final values of  $(t, r)$ , and the result is:

$$\frac{\gamma}{E_a} \exp\left(-\frac{E_a}{\gamma}r_0\right) \left( \exp\left(\frac{E_a}{\gamma}r\right) - \exp\left(\frac{E_a}{\gamma}r_i\right) \right) = v_{\infty}(t - t_i) \quad (\text{S14})$$

By rearranging equation (S14) to find  $r$  as a function of  $t$ , we have Eq. 6.

### D. THE ELECTRIC FIELD IN THE FILM FROM COMSOL SIMULATIONS

We used the finite element method of COMSOL Multiphysics to simulate the electric field due to the AFM tip. The AFM tip is defined as a sphere and a truncated cone (Fig. 3S). In the simulation, the cone height is 800nm, the half angle of the cone,  $20^\circ$ , the width of the film and substrate, 1400 nm, the dielectric constants of the barium titanate (BTO) film<sup>5</sup>,  $\epsilon_x = 4000, \epsilon_y = 4000, \epsilon_z = 200$  and the dielectric constant of the material around the tip, 1. The tip and substrate were taken as "terminals" with the voltage of 0 V and 7 V respectively. Since there are reports<sup>2-4</sup> on the presence of an ultrathin dielectric surface layer (carbon compounds) on ferroelectric materials, 0.5 nm dielectric layer with the dielectric constant of 2 was considered on the films. We simulated the electric field for 2, 10, and 40 nm films and two different tip apex radii of 30 nm and 60 nm. The mesh was selected based on no change in simulation with selection of a finer mesh size.

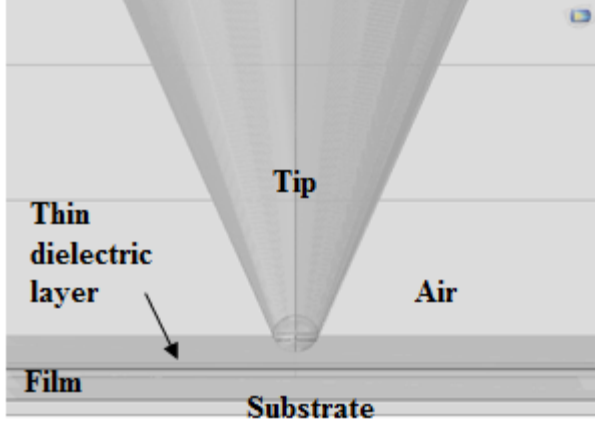


FIG. S3. Defined elements in COMSOL simulation.

The simulation shows that the electric field in the  $z$ -direction under the tip is larger near the surface of the film ( $z = 0$ ) and decreasing moving toward the substrate ( $z = -10$  nm). This is observed in Fig. S4 by comparing the slope of the electric potential vs  $z$  at  $z = 0$ , to the slope at  $z = -10$  nm, for a 10 nm film at  $r = 0$  and  $r = 10$  nm. However, the electric field becomes uniform for larger  $r$  as shown by the simulated data at  $r = 100$  nm for a 10 nm film in Fig. S4.

The electric field in the  $z$ -direction at the surface of the films ( $z = 0$ ) for different films are compared in Fig. S5 indicating the behavior of the electric field as a function of lateral distance,  $r$ , for different thicknesses of the film. The electric field is clearly larger for thinner films than thicker films at  $r = 0$ . However, this order changes at  $r = 50$  nm and the electric field becomes bigger for thicker films due to the greater fringing field from the tip hemisphere compared to thinner films. At larger distances, however, the electric field in thicker films approaches the electric field of thinner film, becoming thickness independent. As discussed in the paper, the COMSOL simulation was used to further support using Eq. 5, the electric field due to the cone, for the electric field at lateral distances larger than about tip diameter.

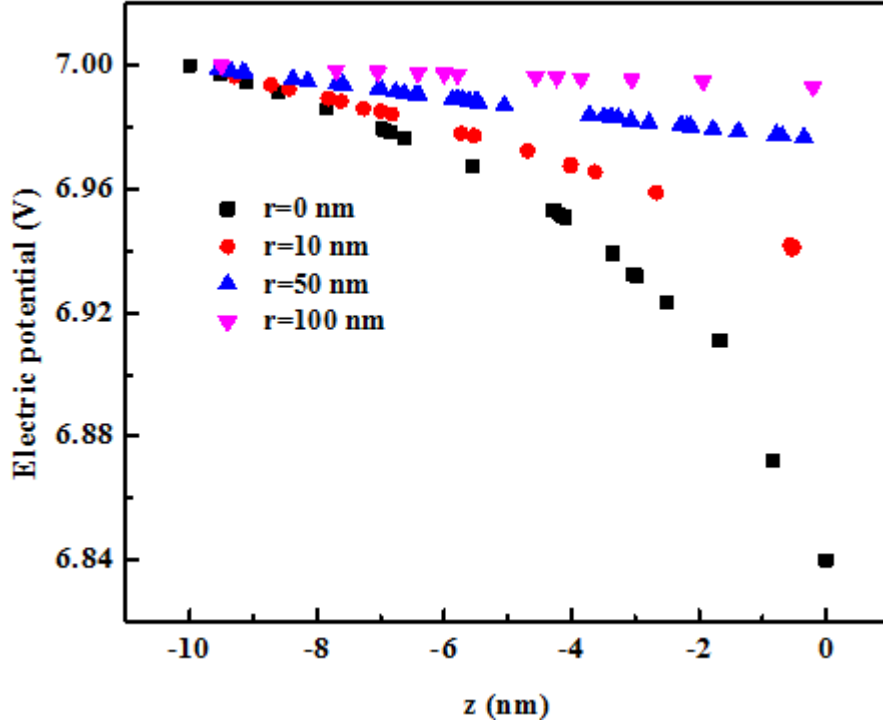


FIG. S4. Electric potential vs.  $z$  for the 10 nm film at different radial distances ( $r = 0$ ,  $r = 10$  nm,  $r = 50$  nm and  $r = 100$  nm) using tip#1.

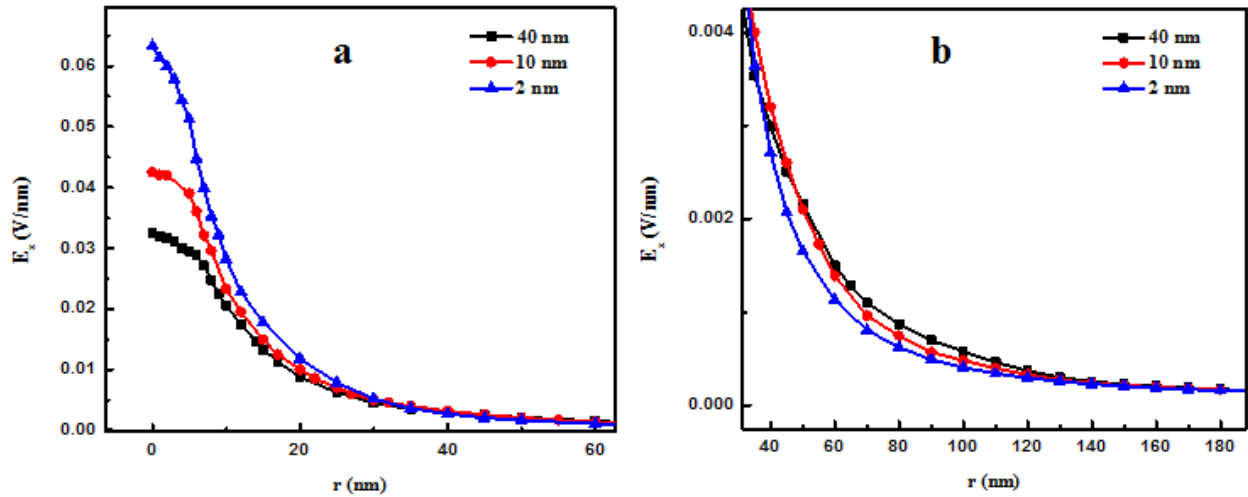


FIG. S5. Simulated vertical electric field at the surface of the films induced by AFM tip#1 in 2,10, and 40 nm films vs. lateral distance from the tip,  $r$  for (a)  $0 \text{ nm} < r < 60 \text{ nm}$ , (b)  $40 \text{ nm} < r < 180 \text{ nm}$ .

## REFERENCES

- <sup>1</sup>B. Wang and C. Woo, “Atomic force microscopy-induced electric field in ferroelectric thin films,” *Journal of Applied Physics* **94**, 4053–4059 (2003).
- <sup>2</sup>Y. TOMASHPOLSKI, E. LUBNIN, and M. SEVOSTIANOV, “Auger-spectroscopy of surface-layers in ferroelectrics,” *Ferroelectrics* **22**, 785–786 (1978).
- <sup>3</sup>J. Baniecki, M. Ishii, K. Kurihara, K. Yamanaka, T. Yano, K. Shinozaki, T. Imada, and Y. Kobayashi, “Chemisorption of water and carbon dioxide on nanostructured batio<sub>3</sub>-srtio<sub>3</sub>(001) surfaces,” *Journal of Applied Physics* **106** (2009), 10.1063/1.3169654.
- <sup>4</sup>F. Peter, K. Szot, R. Waser, B. Reichenberg, S. Tiedke, and J. Szade, “Piezoresponse in the light of surface adsorbates: Relevance of defined surface conditions for perovskite materials,” *Applied Physics Letters* **85**, 2896–2898 (2004).
- <sup>5</sup>F. Jona and G. Shirane, *Ferroelectric crystals* (Dover Publications, New York, 1993) pp. x, 402 pages.